Acta Biomaterialia xxx (2016) xxx–xxx

Contents lists available at ScienceDirect

Acta Biomaterialia

journal homepage: www.elsevier.com/locate/actabiomat

Full length article

Human placenta hydrogel reduces scarring in a rat model of cardiac ischemia and enhances cardiomyocyte and stem cell cultures ☆

Michael P. Francis [a,b,*], Erick Breathwaite [a], Anna A. Bulysheva [c], Frency Varghese [c,d], Rudy U. Rodriguez [a], Sucharita Dutta [b], Iurii Semenov [c], Rebecca Ogle [a], Alexander Huber [a], Alexandra-Madelaine Tichy [e], Silvia Chen [a], Christian Zemlin [c,d]

[a] LifeNet Health Institute of Regenerative Medicine, Virginia Beach, VA, United States
[b] Eastern Virginia Medical School, Norfolk, VA, United States
[c] Frank Reidy Research Center for Bioelectrics, Old Dominion University, Norfolk, VA, United States
[d] Department of Electrical and Computer Engineering, Old Dominion University, Norfolk, VA, United States
[e] FH Campus Wien, Applied Life Sciences, Wien, Austria

ARTICLE INFO

Article history:
Received 27 August 2016
Received in revised form 7 December 2016
Accepted 9 December 2016
Available online xxxx

Keywords:
Placenta
Extracellular matrix
Ischemia
Cardiomyocyte culture
Hydrogel
Decellularized

ABSTRACT

Introduction: Xenogeneic extracellular matrix (ECM) hydrogels have shown promise in remediating cardiac ischemia damage in animal models, yet analogous human ECM hydrogels have not been well development. An original human placenta-derived hydrogel (hpECM) preparation was thus generated for assessment in cardiomyocyte cell culture and therapeutic cardiac injection applications.
Methods and results: Hybrid orbitrap-quadrupole mass spectrometry and ELISAs showed hpECM to be rich in collagens, basement membrane proteins, and regenerative growth factors (e.g. VEGF-B, HGF). Human induced pluripotent stem cell (iPSC)-derived cardiomyocytes synchronized and electrically coupled on hpECM faster than on conventional cell culture environments, as validated by intracellular calcium measurements. *In vivo*, injections using biotin-labeled hpECM confirmed its spatially discrete localization to the myocardium proximal to the injection site. hpECM was injected into rat myocardium following an acute myocardium infarction induced by left anterior descending artery ligation. Compared to sham treated animals, which exhibited aberrant electrical activity and larger myocardial scars, hpECM injected rat hearts showed a significant reduction in scar volume along with normal electrical activity of the surviving tissue, as determined by optical mapping.
Conclusion: Placental matrix and growth factors can be extracted as a hydrogel that effectively supports cardiomyocytes *in vitro*, and *in vivo* reduces scar formation while maintaining electrophysiological activity when injected into ischemic myocardium.

Statement of Significance

This is the first report of an original extracellular matrix hydrogel preparation isolated from human placentas (hpECM). hpECM is rich in collagens, laminin, fibronectin, glycoproteins, and growth factors, including known pro-regenerative, pro-angiogenic, anti-scarring, anti-inflammatory, and stem cell-recruiting factors. hpECM supports the culture of cardiomyocytes, stem cells and blood vessels assembly from endothelial cells. In a rat model of myocardial infarction, hpECM injections were safely deliverable to the ischemic myocardium. hpECM injections repaired the myocardium, resulting in a significant reduction in infarct size, more viable myocardium, and a normal electrophysiological contraction profile. hpECM thus has potential in therapeutic cardiovascular applications, in cellular therapies (as a delivery vehicle), and is a promising biomaterial for advancing basic cell-based research and regenerative medicine applications.

☆ Part of the Special Issue on Extracellular Matrix Proteins and Mimics, organized by Professor Katja Schenke-Layland.

* Corresponding author at: 700 West Olney Rd., Norfolk, VA 23507, United States.
E-mail addresses: mpf3b@virginia.edu (M.P. Francis), erick_breathwaite@lifenethealth.org (E. Breathwaite), abulyshe@odu.edu (A.A. Bulysheva), fvarg001@odu.edu (F. Varghese), rudy_rodriguez@lifenethealth.org (R.U. Rodriguez), duttasm@evms.edu (S. Dutta), Rebecca_ogle@lifenethealth.org (R. Ogle), alexander_huber@lifenethealth.org (A. Huber), czemlin@odu.edu (C. Zemlin).

http://dx.doi.org/10.1016/j.actbio.2016.12.027
1742-7061/

1. Introduction

Regenerative medicine-related therapeutic approaches to heart disease have ranged from the use of cellular and gene therapies, to complex extracellular matrix (ECM) hydrogel injections, each with varying degrees of success [1]. Cell therapy with cardiac progenitor cells injections, for example, has shown early promise [2–4]. However, cellular therapy studies show injected cells alone may not remain at the injection site long-term [5,6], suggesting that cells may act by mechanisms unrelated to the maintenance and long-term function, integration, or survival of the cells at the injection site. Rather, injected cells seemingly act via a paracrine effect, via growth factor secretions and extracellular matrix remodeling events [7,8]. If growth factor or ECM remodeling-related effects are in fact the causative therapeutic agent in myocardial cell therapies, alternative therapeutic approaches may be possible clinically that are more defined, reproducible, and controllable, which may provide a better treatment option compared to use of extraordinarily complex and thus far poorly defined cellular therapeutic strategies.

One such an alternative approach is seen in the delivery of ECM extracts to the ischemic heart, without the additional introduction of cells [9,10]. The use of ECM from the heart (from pericardium or myocardium) or as extracted from the Engelbreth-Holm-Swarm tumor [11] has surprisingly shown effectiveness in reducing damage from cardiac ischemia, including a reduction in scar formation, improved animal survival and overall health. These materials, derived from porcine and murine tissue origins, while effective in rodent and porcine ischemia models, have concerns of transmitting xenozoonoses clinically. Non-human animal tissues also poses risks of immune rejection from the cellular debris, or foreign (possibly tumorigenic) DNA, and also immunogenic epitopes remaining in any decellularized matrix of non-human animal tissue, such as alpha-galactosyl [12,13]. Such foreign material, if injected into the human heart, may stimulate immune reactions that further degrade cardiac health. These risks would be avoidable if the ECM hydrogels were produced from quality controlled, pathogen-screened human tissues with minimal cellular debris (e.g. DNA). Attempts to produce hydrogel from human myocardium have been made, however they failed to form gels and did not appear to persist at the injection sites [14,15], thus limiting clinical utility.

A human placenta tissue-derived ECM hydrogel biomaterial for cardiovascular cell culture and potential therapeutic applications was therefore designed and tested in this work, presenting a clinically-relevant material source from an abundantly available human donor tissue. ECM and growth factor-rich placenta-derived therapeutics (e.g. amniotic dressings) have been used clinically as a matrix to induce cellular migration and proliferation [16] and have been shown to promote the wound healing process [17]. Placenta tissue has been shown to act to reduce inflammation [18] and prevent scar tissue formation [19], while also being non-immunogenic [20]. Placenta products have been used clinically as wound dressings in the eye, heart, skin, bone, and other indications [17,19–23]. However, the use of a placenta-derived ECM preparation formulated as a hydrogel for applications *within* the heart for possibly treating and remediating ischemic injuries, along with use for human cell culture and additional applications, has yet to be explored.

2. Materials and methods

2.1. Extracellular matrix (ECM)

Human placentas were procured from 9 donors with research authorization through LifeNet Health's organ and tissue procurement service and stored frozen. Whole chorionic plate was ground, washed in water, then decellularized for 16–24 h using 2% N-lauryl sarcosine (Sigma Aldrich, St. Louis, MO). Detergent and cell debris was eluted in water with exchanges every hour until clear, after which a sample was taken for gross histological analysis with H&E staining to validate cell removal (processed at Bons Secours DePaul Medical Center, Norfolk, Virginia). The decellularized tissue was then collected by centrifugation at 500*G*, homogenized in 0.1 M hydrochloric acid with pepsin (Sigma-Aldrich, St. Louis, MO) and digested for 64–72 h, followed by irreversible inactivation of the pepsin at pH 8.0. The resulting liquid product of human placenta extracellular matrix (hpECM) was confirmed to form a gel at 37 °C while remaining liquid from room temperature to 4 °C. The total protein concentration in the hpECM was determined by the modified Lowry Protein Assay Kit (Pierce, Grand Island, NY) as described by the manufacturer's recommendations. The final hpECM preparations were confirmed to be free from mycoplasma (MycoAlert™ Plus, Lonza), contained <0.5 EU/ml of endotoxin (PyroGene™ Recombinant Factor C Endotoxin Detection Assay kit, Lonza), assessed for residual DNA contamination by Quant-iT PicoGreen™ (ThermoFisher Scientific, Carslbad, CA), with all tests performed per manufacturer instructions. Lots were also tested for sterility by direct liquid media inoculations.

For use, hpECM preparations were thawed on ice at 4 °C overnight or at room temperature for approximately an hour, then diluted in phosphate buffered saline to normalize protein concentrations (5 mg/ml). Liquid hpECM was handled without the use of pre-chilled tools and equipment and used immediately to prepare hydrogels (formed at 37 °C for 15–30 min in a humidified incubator with 5% CO_2), or used for cell delivery experiments in liquid form then cast at 37 °C after delivery. Cast hydrogels were used immediately for cell culture experiments or stored for further analysis. Other ECM substrates including Matrigel® Basement Membrane Matrix HC (354262, Corning Life Sciences, Tewksbury MA), fibronectin (F2006, Sigma Aldrich, St. Louis MO), and gelatin (G1890, Sigma Aldrich, St. Louis MO) were used according to manufacturer's recommendations.

2.2. Mass spectrometry

Protein concentration of hpECM was determined using a DTT compatible BCA assay (Thermo Fisher Scientific, San Jose CA) and 100 μg of extracted protein sample was run on a NuPAGE reducing gel (4–12% Bis-Tris Gel) (Life Technologies, Carlsbad CA) with NuPAGE MOPS SDS 1X buffer run at 200 V for about 10 min. The remaining protocol for complex protein clean up; protein alkylation with Iodoacetamide; protein cysteine bond reduction via Dithiothreitol and trypsin digestion was carried out following published protocols from our group [24]. Post tryptic digestion, peptides were analyzed on the Q-Exactive (Thermo Fisher Scientific, Waltham, MA) mass spectrometer as described previously [24].

Data informatics on the sample was carried out by applying the label-free precursor ion detection method (Proteome Discoverer, version 1.3, Thermo Fisher Scientific, Waltham, MA). The Sequest algorithm was used to identify peptides from the resulting MS/MS spectra by searching against the combined Human Protein Database (a total of 28,000 sequences) extracted from Swissprot (version 57) using taxonomy "Human." Searching parameters for parent and fragment ion tolerances were set as 15 ppm and 60 mmu for the Q-Exactive MS. Other parameters used were a fixed modification of carbamidomethylation–Cys, variable modifications of Phosphorylation (S,T,Y) and oxidation (Met). Trypsin was set as the primary protease and pepsin was set as the secondary cleavage enzyme since we used this enzyme in our workflow to generate the original biological material. We considered a maximum of 2 missed cleavages. Only those proteins that had >2 peptides identified (or >50% of protein covered by peptides) were included in the

Please cite this article in press as: M.P. Francis et al., Human placenta hydrogel reduces scarring in a rat model of cardiac ischemia and enhances cardiomyocyte and stem cell cultures, Acta Biomater. (2016), http://dx.doi.org/10.1016/j.actbio.2016.12.027

Table 1
ECM-related proteins and growth factors in hpECM preparations as determined by mass spectrometry (n = 3).

Extracellular Matrix Proteins	Growth Factors
• Aggrecan	• EGF
• Agrin	• EGFL-7
• Chondroitin Sulfate Proteoglycan	• FGFs 2,9,12,19,20
• Collagens I, III, IV, VI, XII, XIII, XIV, XIX, XX, XXVIII	• HGF
• Elastin	• iFGFs -12,-13
• Fibrinogen	• IGF-II
• Fibronectin	• PDGFs A,B,C,D
• Ficolin-2	• TGF-β
• Heparin Sulfate Proteoglycan	• VEGFs A,B,C,D
• Laminins α1, α2, α3, α5, β1, β2, γ1, γ3	
• Nidogen	
• Osteopontin	
• Vitronectin	

comparative quantitative analysis steps. The false discovery rate was set at 5% for decoy database searches. Peptides that have yet to be definitively linked to a protein were excluded from further analysis.

Post protein digestion with pepsin enzyme which cleaves preferentially after the N-terminal of aromatic amino acids such as phenylalanine, tryptophan and tyrosine; the entire sample was digested with trypsin under protein reduced/alkylated conditions. The peptides from the initial pepsin cleavage were not separated from the peptides undergoing trypsin cleavage at any point in time. The peptides resulting from both the pepsin and trypsin cleavage formed a homogeneous mixture of peptides that were subjected to peptide identification for Table 1. The data acquisition was performed under high mass accuracy conditions.

Data analysis was performed in two separate stages; for stage 1, trypsin alone was considered as the proteolytic enzyme of choice. From this search, peptide fragmentation pattern was matched to the proteins from Table 1 via probability dependent data base searches against the human database. For stage 2, trypsin was combined with pepsin for additional searches from the peptide fragmentation spectra to confirm the presence of proteins in Table 1. Since sequence information from trypsin searches alone matched the proteins from Table 1, we conclude that intact forms of the proteins listed in Table 1 were present in the mixture.

2.3. Enzyme-linked immunosorbent assays (ELISAs)

Enzyme-linked immunosorbent assays (ELISAs) were used to determine the collagen I (Chondrex, Richmond WA), collagen IV (Echelon, Salt Lake City UT), laminin (EMD Millipore, Billerica MA), fibronectin (EMD Millipore, Billerica MA), and placental lactogen (Genway Biotech, San Diego CA) in hpECM hydrogels, with all tests performed per manufacturer's specifications.

2.4. Scanning electron microscopy (SEM)

SEM analysis was performed using a JEOL JSM-6060LV at Jefferson Labs (Newport News, VA). Ethanol fixed/dehydrated hpECM hydrogels from two independent preparations were sputter coated with gold for high-resolution SEM imaging (15 kV).

2.5. Cardiomyocyte cell culture

Human adult cardiomyocytes (Celprogen, Torrance, CA) were seeded at 10,000 cells/cm^2 on Celprogen extracellular matrix coated plates in serum-free and xeno-free media (also from Celprogen). After culturing the cells for a week at 37 °C with 5% CO_2, with daily media changes, the cells were transferred to 3 unique lots of hpECM, 0.1% gelatin, tissue culture plastic, or Matrigel®. At day 1, 3, 5, and 7 of culture with daily media changes, cell viability/metabolic activity was assessed using alamarBlue® (Abd Serotec, Kidlington, UK), per manufacturer's specifications, with 2 h incubations of the dye. Fluorescence was read on a Fluoroskan Ascent™ FL plate reader.

Additionally, cardiomyocytes differentiated from induced pluripotent stem cells (iPSCs) from Cellectis (Gothenburg, Sweden) were grown on hpECM hydrogels and compared to gelatin, fibronectin, Matrigel®, and tissue culture plastic. Cells were cultured in Cardiomyocyte Culture Base Medium (Cellectis, Gothenburg, Sweden) supplemented with Y27632 dihydrochloride (Sigma Aldrich, St. Louis, MO) and 10% FBS. The cells were incubated at 37 °C with 5% CO_2. Plates were observed initially over the first hour and then twice daily for signs of cell attachment, contractions, and synchronized beating across the well. After 30 days in culture, the cells were fixed in 4% PFA for immunohistochemistry analysis.

2.6. Measurements of intracellular Ca^{2+} concentration

The detailed procedures utilized for loading iPSC-derived cardiomyocytes with Fura-2 and dye calibration were reported previously [25]. Detailed methods are provided in Supplemental Materials.

2.7. Catheter delivery of hpECM with adipose stem cells (ASCs)

ASCs were cultured and acclimated for a week in serum-free and xeno-free conditions using StemPro® MSC SFM (Thermo Fisher, Carlsbad CA), for subsequent catheter injection through a 6 French cardiac catheter along with hpECM, to assess cell viability in a simulated minimally invasive surgically delivery approach. 400,000 ASCs were delivered onto a culture plate, as delivered either with a pipette, or in a catheter with StemPro media alone, or with cells premixed with 1.0 ml of hpECM for delivery through the cardiac catheter to the culture well. Cell morphologies were monitored and cell viability was assessed over 5 days with alamarBlue® according to manufacturer's recommendations.

2.8. Human umbilical vein endothelial cell (HUVEC) culture on hpECM

HUVECs (LifeTechnologies, Carlsbad, CA) grown in Medium 200 (LifeTechnologies) media supplemented with Low Serum Growth Supplement (Life Technologies) were transferred to 24 well plates pre-coated with HuECM, Matrigel® or tissue culture plastic directly at a density of 100,000 cells per well. 500 μL of media was added to each well. About 18 h after plating, the cells were incubated with calcein AM (Life Technologies) diluted in DPBS at a concentration of 2 μg/ml, and imaged for endothelial tube formation under fluorescent light (Zeiss Axiovert), with subsequent branching points quantitation using ImageJ FIJI (NIH shareware).

2.9. Rat acute myocardial infarction model

Animal experiments in this study were conducted in accordance to an approved Old Dominion University Institutional Animal Care and Use Committee protocol. Studies were conducted in an AAALAC accredited facility. Twenty adult male Sprague Dawley rats (546 ± 21 g at time of surgery) were purchased from Harlan Laboratories (Indianapolis IN). Animals were allowed at least a 48-h acclimatization period. Induction of anesthesia was initiated with 3–4% isoflurane inhalation and an intramuscular injection of acepromazine at 1 mg/kg. Intubation was performed with a 16G intravenous catheter, and animals were ventilated with a volume-controlled ventilator at 8–10 ml/kg tidal volume at 70 breaths per minute. Isoflurane (2–3%) was used to maintain anes-

Please cite this article in press as: M.P. Francis et al., Human placenta hydrogel reduces scarring in a rat model of cardiac ischemia and enhances cardiomyocyte and stem cell cultures, Acta Biomater. (2016), http://dx.doi.org/10.1016/j.actbio.2016.12.027

thesia. A heating pad placed underneath the animal was used to support body temperature throughout the procedure. Animals received a prophylactic 14-day antibiotic course of trimethroprim sulfate at 0.5 mg/kg daily and sterile technique was utilized to prevent infection. Seven animals died intraoperatively, before injections and likely as a result of the LAD ligation and resulting ischemia and fibrillations that followed, and were not included in later analyses. Only animals that survived 2-days post-LAD ligation surgery (7 Saline Injection, 6 hpECM injection) were included in this study for further analyses.

The heart was surgically exposed with a left thoracotomy at the fifth intercostal space. Pericardial removal exposed the left anterior descending (LAD) coronary artery. LAD coronary artery occlusion was performed with a 5–0 silk suture to induce ischemia in the distal regions of the left ventricular myocardium. Observation of blanching of the myocardium was used to confirm induction of ischemia. Treatment with hpECM or sham (saline) injections was initiated thirty minutes after the induction of ischemia, allowing for a degree of cardiomyocyte death in the ischemic region prior to injection. During this time, the thoracic cavity was left exposed, but covered with moist gauze to minimize dehydration and infection. Following injections, the thoracic cavity was closed with 4–0 Vicryl suture. The lungs were momentarily fully inflated to expel any air trapped in the thoracic cavity prior to sealing the cavity to prevent pneumothorax. The remaining muscle, connective and skin layers were then also closed separately with 4–0 Vicryl suture in an interrupted pattern. Animals were allowed to recover and were monitored postoperatively until ambulatory. Postoperative pain was controlled with carprofen and buprenorphine for up to 48 h or until no longer needed. To further validate induced ischemia in hpECM and saline injected animals, echocardiography was performed (Methods in Supplemental data).

2.10. Treatment of ischemic myocardium

hpECM preparations were placed on ice at 4 °C until fully thawed and adjusted to a final total protein concentration of 5 mg/ml. Thirty minutes' post-ligation, three injection sites in the ischemic myocardium were chosen based on the location of blanching, indicating the ischemic region. Each treatment site received 25 µl of hpECM dilution for a total of 75 µl per treatment site. No backflow of hpECM following the removal of the syringe needle form the injection site was observed. The sham control group received vehicle only injections of 0.9% saline as per the aforementioned injection strategy.

2.11. In vivo gelation analysis

hpECM was biotin conjugated using the EZ-Link Sulfo-NHS-biotin kit (Life Technologies, Carlsbad CA) as per manufacturer's instructions. Myocardial ischemia was induced as described above in two rats. Biotin labeled hpECM was injected into ischemic regions of the left ventricular myocardium as described above. One hour after biotinylated hpECM injections, rats were euthanized and hearts were collected for histological analysis. Hearts were fixed in 4% paraformaldehyde, flash frozen in optimal cutting temperature compound (Tissue-Tek® OCT, VWR), cryosectioned to 8 µm sections, and mounted on slides. Adjacent serial sections were either stained for collagen with Serius Red/Fast Green, or for Biotin with FITC-conjugated Streptavidin. hpECM gelation was evaluated based on presence of both collagen staining and biotin staining, as confirmed to be co-localized in consecutive sections, with staining performed per the Supplemental methods.

2.12. Optical mapping

Eight weeks after the initial surgery, hearts were extracted and were ensured to have a complete ligation of the LAD by perfusing food coloring through the cannulated aorta (8 of 10 passing), and their electrical activity was analyzed subsequently with optical mapping as described previously [26,27], with detailed methods provided in the Supplemental Materials.

2.13. Histology

At the conclusion of optical mapping, hearts were stained with triphenyltetrazolium chloride (TTC, Sigma-Aldrich, St. Louis MO). Specifically, TTC was dissolved in PBS 1%W/V to replace the Tyrode solution. The heart was perfused with TTC for 15 min and preserved in formalin for sectioning. The hearts were then sliced every 2 mm from the apex to 2 mm above the suture. Serial heart slices were embedded in paraffin, sectioned every 7 mm, mounted and stained with Mason's Trichrome and H&E by VCU Pathology Services (Richmond, VA). Scar volume was determined, as assessed double-blinded, by tracing and volumetric calculations using ImageJ to derive the scar size in each group, with both blind measurements and analysis performed.

2.14. Echocardiography

To confirm induction of an ischemic event, echocardiography was performed 2 days prior to the surgery and twice post-surgery, at 4 weeks and 8 weeks, on all control and hpECM-treated rats, using a Vevo-770 (VisualSonics) with a 13–23 MHz non-linear array transducer. Each rat was anesthetized with 1.5–2.0% isoflurane by mask, the chest was shaved, the animal was laid in the supine position on a warming pad. Two-dimensional M-mode and B-mode data were recorded in parasternal short axis. All echocardiogram measurements were performed using the same equipment and software, and by the same examiner. The examiner was not aware if the rat under examination was hpECM or sham-treated, and thus blinded in analyses.

2.15. Statistical analyses

Cell culture studies for ASC catheter injection experiments and cardiomyocyte metabolic activity (alamarBlue®) studies were individually tested by one-way analysis of variance (ANOVA) with a Tukey's HSD post hoc test for multiple comparison subsequently performed, with significance considered at $p < 0.05$. Data generated in other cell culture studies were compared with a Two-Way ANOVA followed by Tukey's HSD post hoc test for multiple comparison, with data shown as means ± SEM. The Kaplan Meier test with Cox Proportional Hazards Regression was performed to assess animal survival in the hpECM *versus* saline injected groups over 8 weeks post-infarct. Data generated in the rat functional study were compared with a Wilcoxon-Mann-Whitney test, with data shown as means ± SD. Significance was considered at $p < 0.05$. All statistical analyses were performed using GraphPad Prism 7.

3. Results

3.1. hpECM hydrogel characterization

hpECM preparations were shown to be free of cellular debris and containing minimal residual DNA after processing (Fig. 1A–G). As a final liquid product of extracted placental ECM, hpECM did not require the use of chilled tools and equipment (as was required with Matrigel®), and readily formed a hydrogel at

Please cite this article in press as: M.P. Francis et al., Human placenta hydrogel reduces scarring in a rat model of cardiac ischemia and enhances cardiomyocyte and stem cell cultures, Acta Biomater. (2016), http://dx.doi.org/10.1016/j.actbio.2016.12.027

37 °C in 15 min, a gel which persisted for an average of 27.2 ± 2.1 days in culture (37 °C at 100% humidity), as validated in n = 24 separate experiments that monitored initial gelation every 5 min for the first hour, and assessed gel stability over 30 days. The hpECM preparations were used successfully in thin coating of tissue culture labware, thin and thick gel hydrogel preparations, and the casting of robust 3dimensional (3D) hpECM hydrogels. 3D hpECM hydrogels retained the dimensions of the gelling vessel and withstood further handling and modification by sharp incision with a scalpel (Fig. 1H,I). SEM revealed the hydrogel's porous, nanofibrous matrix architecture with apparent porous interconnectivity (Fig. 1J).

Four lots of hpECM were further characterized by hybrid quadrupole-orbitrap mass spectrometry and found to be consistently rich in collagens, laminin, fibronectin, glycoproteins, and growth factors, including pro-regenerative, pro-angiogenic, and stem cell-recruiting factors such as VEGF-A, VEGF-B, HGF, bFGF, PDGFs, IGF-II and EGFs (Table 1). hpECM also proved more consistent from lot-to-lot as compared to Matrigel®, with a marked difference in ten of the most frequent protein hits quantified by mass spectrometry. (Supplementary Table 1 and Fig. S3). ELISA quantitation of nine unique hpECM preparations showed an average of 46 ± 7% collagen type I, 3.0 ± 0.4% collagen type IV, 0.3 ± 0.003% laminin gamma-1 chain, and 0.08 ± 0.006% fibronectin relative to total protein content. hpECM was also found to contain on average 257 ± 61 ng/ml of Human Placental Lactogen (a pro-angiogenic growth factor common to the placenta) by ELISA, with these targets chosen for quantitative analysis as they are among the key proteins and growth factors known to be present in the placenta.

3.2. Human somatic cell bioactivity on hpECM hydrogels

Human somatic cardiomyocytes were able to attach and spread on hpECM while showing increasing metabolic activity (related to cell survival and health) over time (Fig. 2A), akin to culture on con-

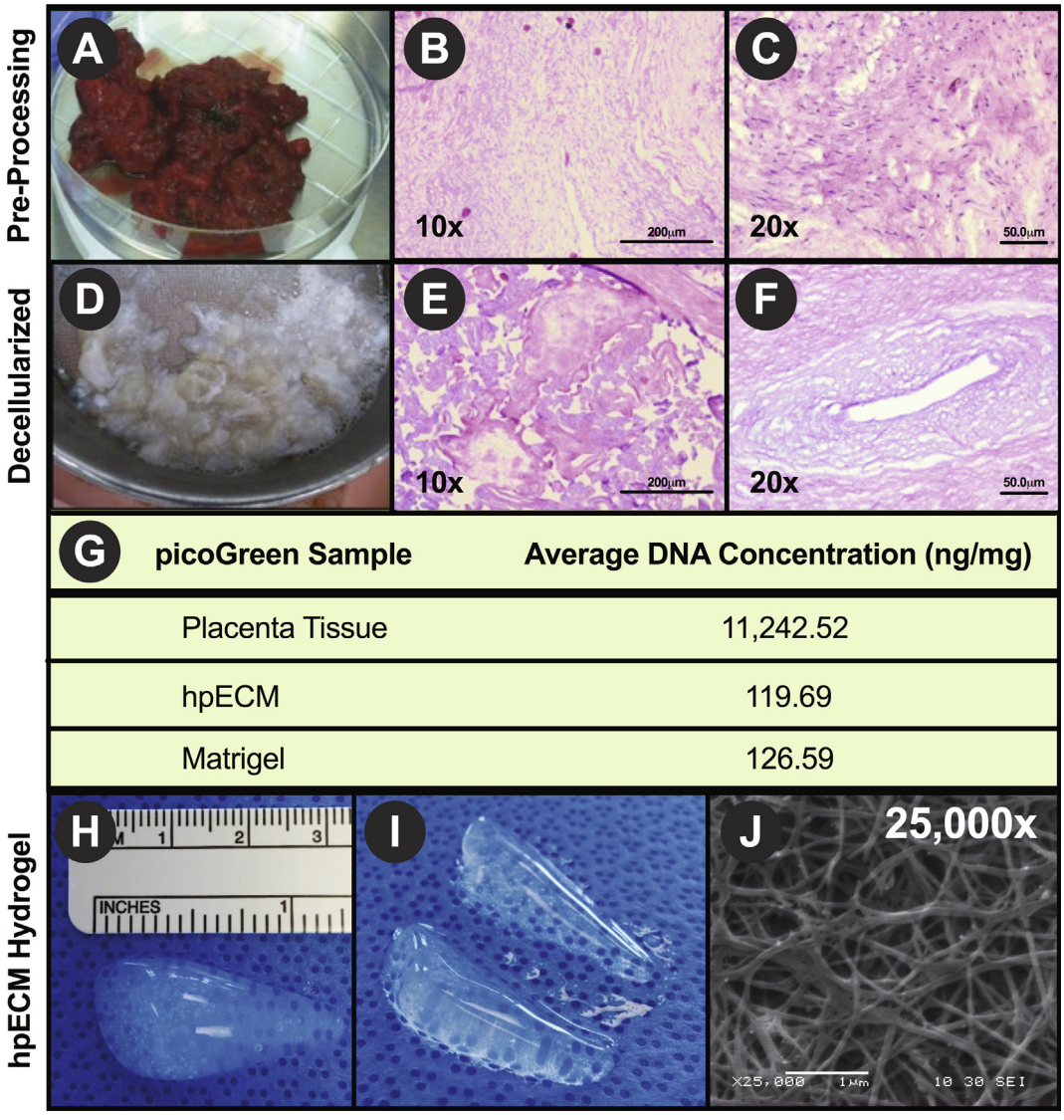

Fig. 1. Placental Tissue Decellularization Confirmation with Macroscopic and Microscopic Appearance of hpECM Hydrogel Product: Placenta is shown pre-processing (A–C) both macroscopically (A) and as microscopic sections stained with H&E (B,C), as compared to post decellularization (D-F) where the tissue appears cleared of blood (D) and also of cellular components (E,F). (G) DNA content in the starting placental tissue compared to the final hpECM product was measured, where a large reduction in DNA is noted compared to the mouse DNA content of Matrigel® (n = 3). (H) Macroscopic appearance of a hydrogel cast for 10 min in a water bath at 37 °C, which maintained its shape following gel sharp dissection (I). (J) SEM of hpECM further revealed the macroporous and nanofibrous features of the 5mg/ml hydrogel, with 143 ± 87nm fiber width on average (from n = 30 fibers measured).

Please cite this article in press as: M.P. Francis et al., Human placenta hydrogel reduces scarring in a rat model of cardiac ischemia and enhances cardiomyocyte and stem cell cultures, Acta Biomater. (2016), http://dx.doi.org/10.1016/j.actbio.2016.12.027

ventional tissue culture substrata, including gelatin and tissue culture plastic (TCP), with two separate lots of hpECM showing signifianctly improved metabolic activity as compared to TCP over seven days of cardiomyocyte culture.

The possibility for delivery of adipose-derived stem cells (ASCs) mixed in the hpECM preparation and delivered *in vitro* via a cardiac catheter (to simulate, *in vitro*, the deployment of cell plus hpECM in a minimally invasive surgery model), was assessed for possible deleterious effects of shearing force via cell delivery in the viscous hpECM hydrogel. The use of hpECM for cell delivery did not significantly impair the ASC metabolic activity over 7 days (Fig. 2B) in this xeno-free and serum-free culture system.

HUVECs were further assessed for growth potential on hpECM. HUVECs underwent branching morphogenesis to form vessels on a hpECM hydrogel in culture, as compared to Matrigel® (Fig. 2C, D). No significant difference in the number of branching points was noted between two hpECM lots and Matrigel®, as compared to HUVECs grown on TCP, which did not show branching.

3.3. Induced pluripotent stem cell-derived cardiomoycyte culture on hpECM hydrogels

Human iPSC-derived cardiomyocytes were tested on hpECM as compared to standard ECM substrates of gelatin and fibronectin. The fetal-like iPSC-cardiomyocytes rapidly attached, contracted, and synchronized faster on hpECM than any other conventional tissue culture substratum tested, with contraction by 8 h and synchronization noted after overnight culture on hpECM, as compared to contraction noted after 2–4 days on Matrigel®, fibronectin, or collagen culture substrates, in repeated tests (representative hpECM Videos 1 and 2). iPSC-cardiomyocytes grown for 4-weeks on hpECM hydrogel and stained for cardiac troponin and GATA4 showed that the iPSCs maintain the cardiomyocyte lineage long-term on hpECM, and further exhibited cell alignment not observed on standard fibronectin-coated cultures (Fig. 3A, B). iPSCderived cardiomyocytes grown on hpECM hydrogels, Matrigel® and fibronectin were further tested for electrical coupling and cell synchronization at 24 h of culture, as indicated in observation of Ca^{2+}-transients across a cell monolayer following electric stimulation (Fig. 3C–E and Video 3). iPSCs-derived human cardiomyocytes grown on fibronectin and Matrigel® did not show response to electrical stimulations in 3 separate attempts. Only cells grown on hpECM allowed for recordings of Ca^{2+}-transients and thus confirmed early contractility, coupling and cell synchronization for human cardiomyocytes grown on hpECM, as quantified 24–30 h after initial cell seeding.

3.4. hpECM injection localization after in vivo injection

Biotin-labeled hpECM hydrogel was injected into the myocardium of live animals and assessed histologically after 60 min to test the delivery and localization of hpECM in the rat heart. Fluorescence microscopy of histologic cross sections showed the presence and retention of labeled hpECM hydrogel filling the extracellular space surrounding the cardiac myofibrils at one-hour post injection under physiological conditions (Fig. 4). In addition, biotin labeled hpECM is localized in the injection sites and notably absent in the un-injected right ventricular control region. The presence of hpECM in the interstitial spaces of the injected myocardium was further confirmed histologically by Sirius Red staining in serial sections with biotin-labeled hpECM (Fig. S1A). In serial sections adjacent to biotin-labeled sections, the presence of Sirius Red stained hpECM was found co-localized with biotin-labeled hpECM, and also present along a spatially defined region proximal to the treatment site, but not within distal areas

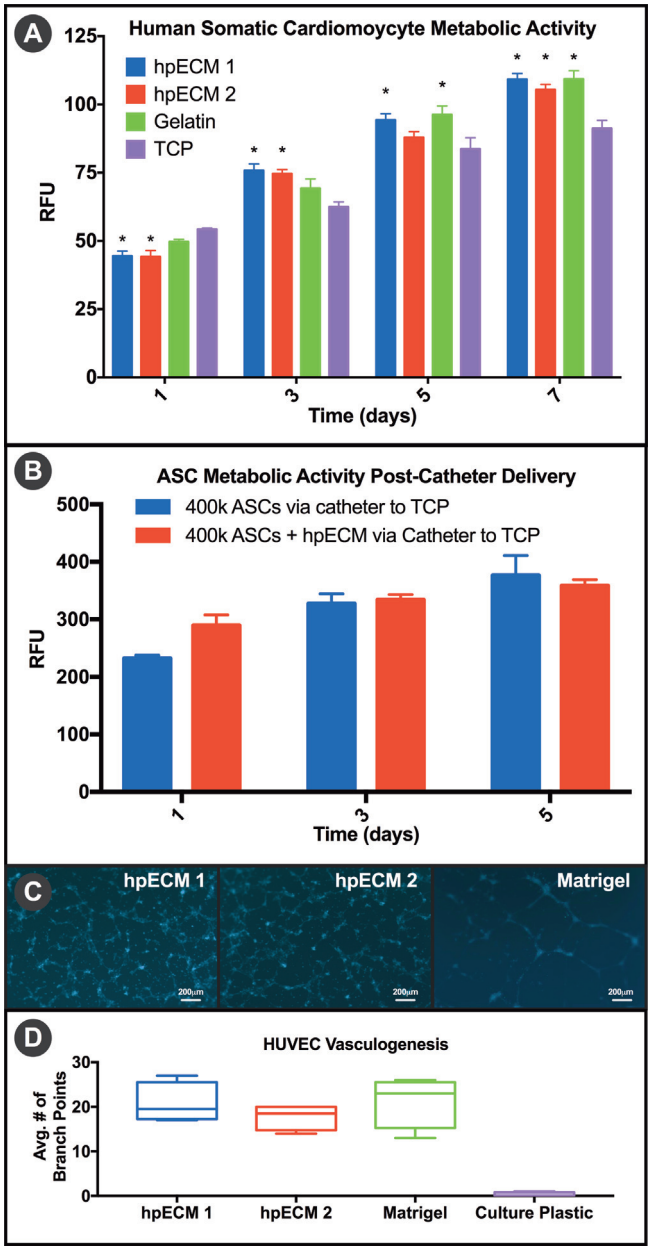

Fig. 2. Culture and Metabolic Activity of Adult Human Cardiomyocyte on hpECM Hydrogels: (A) Through 7 days of culture, hpECM supported metabolic activity (related to survival and proliferation) over time in a similar or significantly higher rate as conventional tissue culture substrata, including gelatin and tissue culture plastic (TCP), suggesting cardiomyocyte health and sustainable culture on human ECM (hpECM) at least comparable to standard materials (n = 3, *denotes statistical significant different as compared to TCP). (B) Cardiac catheter-delivered 400,000 ASCs/ml show, as delivered in media or with hpECM and ASCs mixed in the 3D gel, that use of hpECM as a cell carrier did not negatively affect the metabolic potential, and thus apparent viability, of ASCs as determined by alamarBlue® assay (n = 3, no significant difference between groups at each time point). (C) Human umbilical vein endothelial cells (HUVECs) undergo branching vasculogenesis when placed in or upon a hydrogel of HuECM and Matrigel®, as is seen Calcein AM staining of the tubules imaged by fluorescent microscopy. (D) The number of branching points averaged between groups of two unique batches of HuECM and Matrigel® relative to plastic is also quantified from five fields of view, with no significant difference between hpECM lots and Matrigel®. Statistical significance assed between groups by a two-way ANOVA followed with a Tukey multiple comparison test, with p set at <0.05 for each analysis.

of the same tissue or a treatment site receiving a saline injection (negative controls) (Fig. S1A), validating that the liquid hpECM converts to a stable gel after injection that persists near the injec-

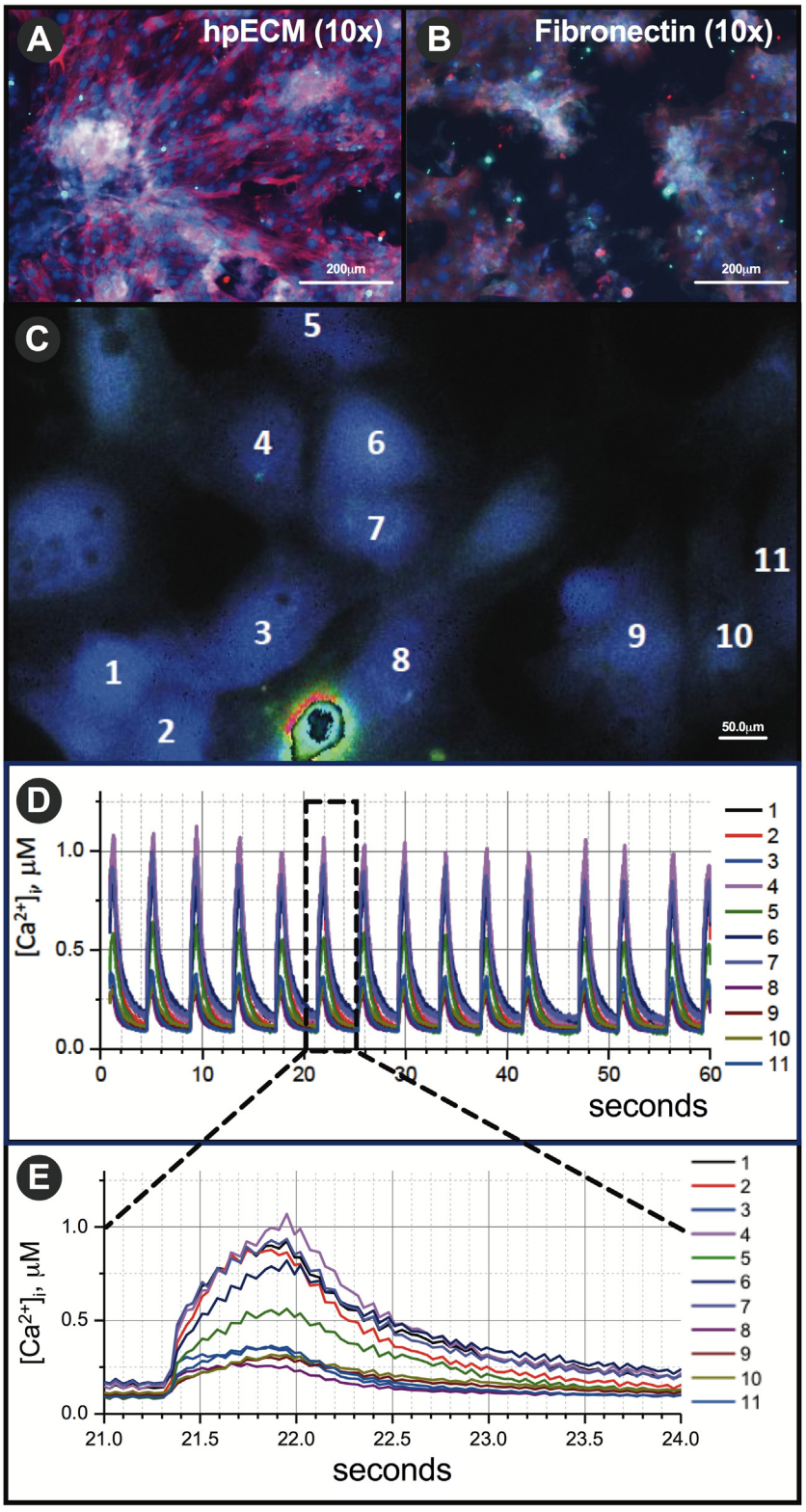

Fig. 3. iPSC-derived Cardiomyocytes Attachment and Electrical Coupling on hpECM Hydrogels: (A) iPSC-derived cardiomyocytes grown on hpECM hydrogel are shown to maintain cardiomyocyte markers and exhibit an intrinsic pattern of cell alignment not observed in conventional tissue cultures on fibronectin (B), where nuclei are labeled blue with DAPI, cardiac troponin is shown in red, and GATA4 is shown in green (representative from n = 6 in triplicate repeats). (C) iPSC-derived cardiomyocytes cultured on 3D hpECM hydrogels displayed interconnectivity and electrical coupling in only 18 h of culture, where cell numbering shown corresponds to fluorescent Ca^{2+} transients for each individual cell as shown over 15 stimulations over 60 s (D), and as isolated across a single, magnified stimulation response (E). (For interpretation of the references to colour in this figure legend, the reader is referred to the web version of this article.)

tion site. hpECM was further confirmed to persist for at least 2 weeks in immune competent mice in a subcutaneous injection model, where hpECM gels were found present macroscopically. H&E stained subcutaneous implants further showed greater apparent cell infiltration as observed microscopically in hpECM compared to Matrigel® at 2 weeks post-injection (Fig. S1B).

Please cite this article in press as: M.P. Francis et al., Human placenta hydrogel reduces scarring in a rat model of cardiac ischemia and enhances cardiomyocyte and stem cell cultures, Acta Biomater. (2016), http://dx.doi.org/10.1016/j.actbio.2016.12.027

3.5. hpECM has no deleterious effect on survival or cardiac output in a rat model

Over the 8 weeks post LAD ligation, only one hpECM injected animal died compared to four that died injected with saline post-infarction. Kaplan-Meier statistical analysis showing no significant change in mortality for hpECM treated animals, supporting its safe use (Fig. 5A). Over 8 weeks the weight (normalized to week zero) of hpECM treated animals increased by 31 g at 4 weeks and another 49 g at 8 weeks, compared to only adding 12 g at four weeks and loosing 63 g at 8 weeks on average for saline injected animals (Fig. 5B). Echocardiography data further showed no deleterious effect of hpECM injection over time, with no statistically significant difference noted between end systolic volume (ESV) (Fig. 5C), end diastolic volume (EDV) (Fig. 5D), ejection fraction (EF) (Fig. 5E), or fractional shortening (FS) (Fig. 5F) between hpECM and sham groups, showing the safe use of hpECM in this model (a xenotransplant). Echocardiography data suggests successful induction of ischemia in hpECM and saline injected animals via altered end systolic volume at 4 weeks in both groups (not significantly different), as evidence of hypertrophy.

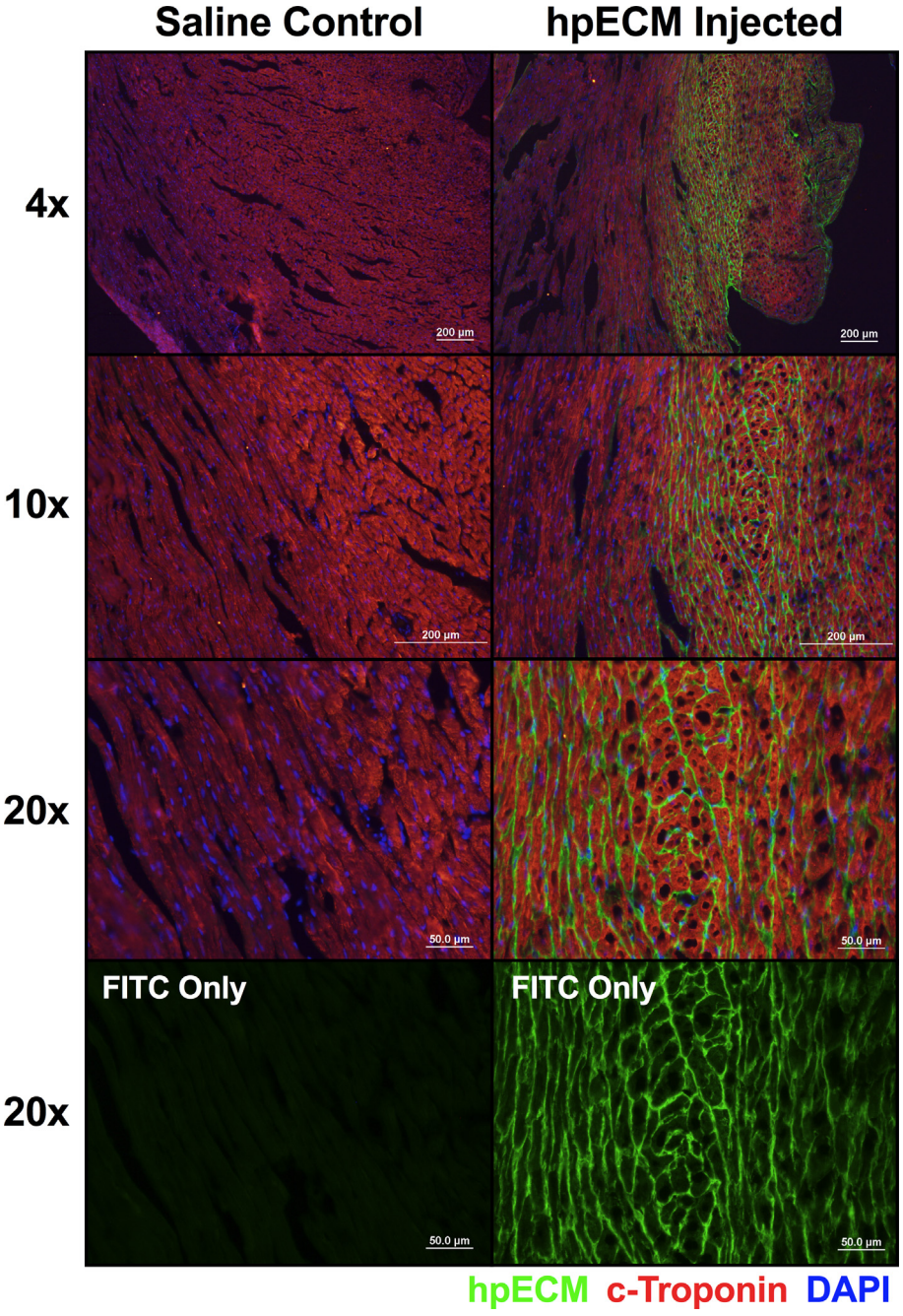

Fig. 4. Localization of Biotin-labeled hpECM Following Injection into the Ischemic Rat Heart: Delivery and localization of the injected placenta hydrogel was validated in the rat myocardium by imaging biotin-labeled hpECM injected into the rat heart after 1 h, as compared to un-injected regions of the right ventricle in the same heart (n = 2). The delivered hpECM (green labeled) is shown by IHC to surround the cardiac troponin labeled (red) myofibrils, and DAPI (blue) labeled cells, suggesting high flow ability in the liquid state prior to gelling, with the placenta ECM being prominently localized at an hour post-injection in the interstitial space, as validated in serial sections stained with Sirius Red (Fig. S1). (Holes in the sections are cryosectioning artifacts). (For interpretation of the references to colour in this figure legend, the reader is referred to the web version of this article.)

Please cite this article in press as: M.P. Francis et al., Human placenta hydrogel reduces scarring in a rat model of cardiac ischemia and enhances cardiomyocyte and stem cell cultures, Acta Biomater. (2016), http://dx.doi.org/10.1016/j.actbio.2016.12.027

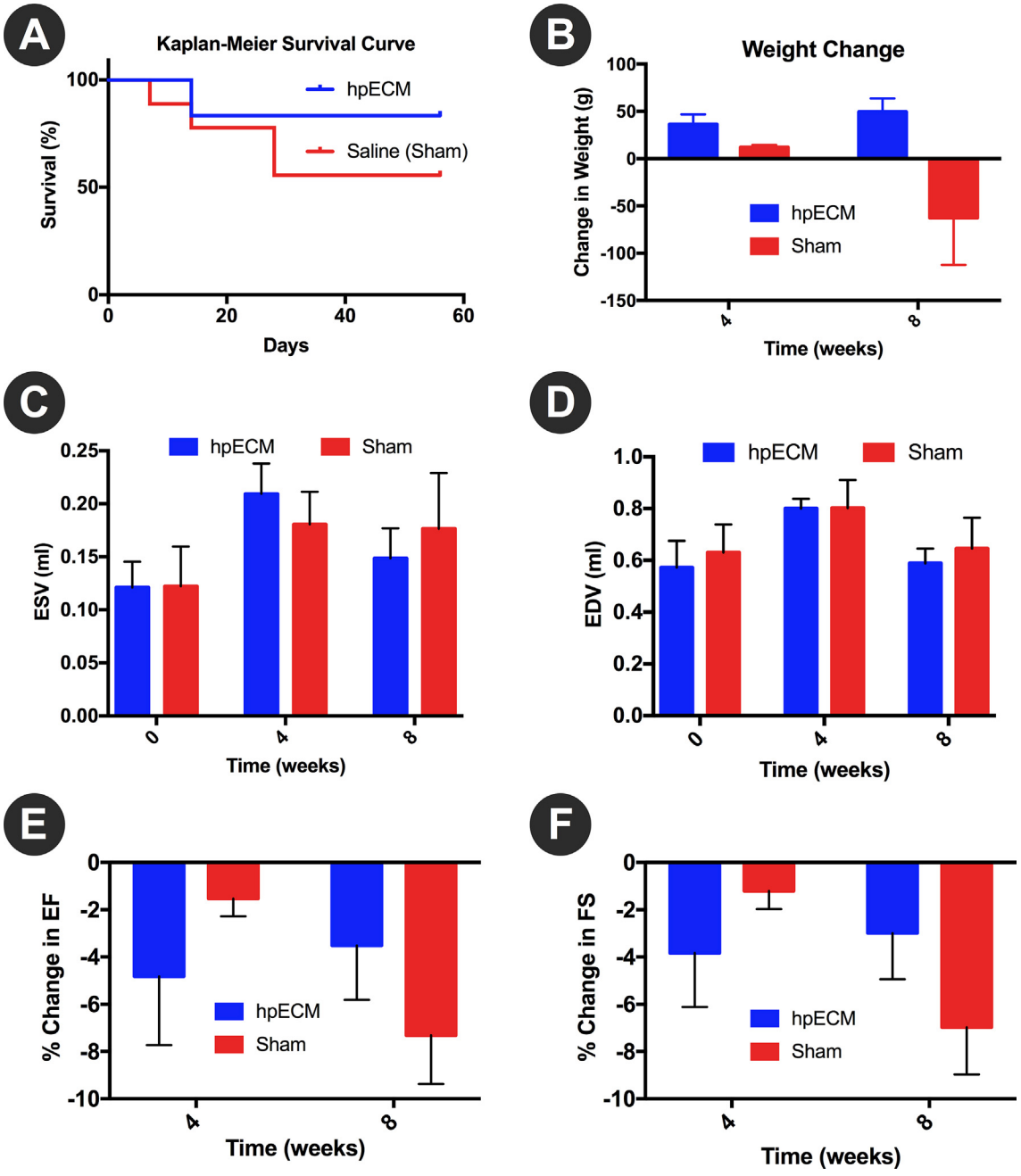

Fig. 5. hpECM Safe Use. Kaplan-Meier Survival Analysis (A) showed no risk of increased mortality with hpECM injection relative so saline, nor was there a significant weight loss in hpECM treated animals (B) relative to saline injected controls. Echocardiography data is shown for the ESV (C), EDV (D), EF (E) and FS (F), where so significant difference was noted over 8 weeks in hpECM treated groups compared to shams, showing safe use of hpECM as injected into the heart.

3.6. hpECM reduces damage from ischemic injury

Post-infarct scar size formation was evaluated in TTC-stained explants and confirmed via gross histologic staining on Mason's Trichrome stained specimen (Fig. 6A,D and representative TTC staining in Fig. S2). Trichrome staining showed larger infracted zones consistently in sham treated animals (dashed circle in Fig. 6A, D). H&E in the infarcted region (Fig. 6B, E, from dotted square region from Fig. 6A, D via serial section) further revealed absence of macrophages or other histological signs of inflammation in hpECM treated animals in the injection region at 8-weeks, along with minimal apparent scar tissue and minimal myofibroblast infiltration in hpECM relative to the sham group, which supports the trichrome data. Blinded measurements and analyses of collagen scar tissue via Mason's Trichrome sections showed hpECM-treated infarcted hearts with a significant reduction in scar size at 8 weeks as compared to sham treated hearts. A statistically significant reduction in the average scar volume in hpECM-treated animals was calculated at $p = 0.0312$ as compared to saline injected sham control animals (Fig. 6C, with measurements made per the diagrammatic representation in Fig. S2). Minimal myocardial wall thinning suggests a mild-to-moderate, rather than an extreme, ischemic event was induced in this animal model.

3.7. hpECM restores cell electrical synchronization in infarcted left ventricular myocardium

Optical mapping revealed further that the surviving tissue in hpECM-treated hearts had normal patterns of electrical activity (Fig. 7). In particular, hpECM-treated hearts showed no areas of

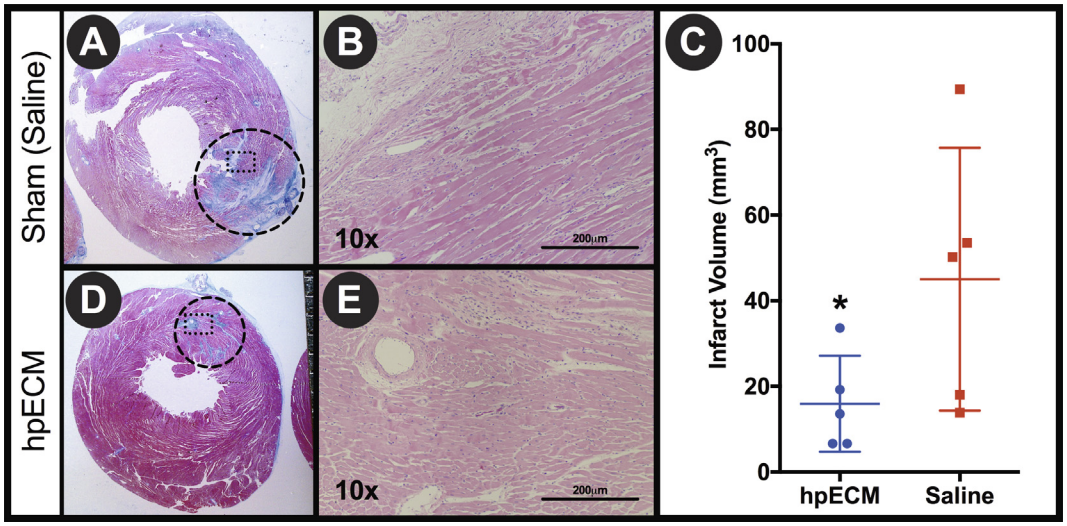

Fig. 6. Reduction in Scar Formation in hpECM-treated Acute Myocardial Infarcts: Representative images of Mason's Trichrome stained hearts from sham (A) and hpECM injected (B) animals show larger blue scar tissue region in sham groups (dashed circle), with H&E from serial sections (taken from the region inside the scarred region as indicated in the dotted square in panels A and D) show scarring and fibroblastic cells in sham sections (B) with less scarring and healthy cardiomyocytes present in hpECM injected tissue (E). (C) The scar volume in hpECM-treated hearts is significantly reduced ($p = 0.0312$) versus saline controls, with $n = 5$ per group, via blinded measuring and analyses of Mason's Trichrome stained serial sections of hear (per the method illustrated in Fig. S2). (For interpretation of the references to colour in this figure legend, the reader is referred to the web version of this article.)

slow conduction or changes in action potential duration in the vicinity of the infarct. Panels 7A-C show photographs of representative no-infarct, infarct-saline, and infarct-hpECM hearts in our setup, including the stimulus electrode and a mark at the stimulation site. Panels 7D-F show activation maps of representative heart in the three groups. In the saline-treated heart (Panel 7E), the smooth transition of activation times in the vicinity of the infarct indicates that the propagation velocity of excitation is approximately constant. Likewise, in the hpECM-treated heart, the propagation of excitation is smooth, and activation is completed after a similar time, indicating a propagation speed close to that of control hearts. There is no propagation block and no area of slow conduction in the vicinity of the infarct, which would manifest as a crowding of isochrones or possibly islands of unexcited tissue. Panels 7G-I show the distribution of action potential durations (APDs) in the three groups in representative hearts. In the hpECM-treated heart, the APDs are quite uniform across the ventricle and there is very little variability (2 ms) of the APD in the direct vicinity of the infarct. An area around the stimulation site with somewhat increased APD (4 ms), which may be related to imaging distortion by the electrode (see Panel 7B); however, there are also larger variations (up to 10 ms) in the non-infarcted control (Panel 7G). All hpECM-treated hearts tested showed activation maps and action potential maps consistent with the representative examples shown here, with no sign of impeded conduction or change in APD around the infarcts.

Panel 7J compares the average local relative variability in conduction velocity in the border zone of the infarct for all saline- and hpECM-treated hearts. High variability in conduction velocity is a sign of discontinuous conduction or conduction block that promotes arrhythmogenesis. We found that the variability of conduction velocity is significantly lower in hpECM-treated hearts than in saline-treated hearts (0.095 ± 0.020 vs 0.184 ± 0.024, $p = 0.036$)(Panel 7J); the variability of conduction velocities in comparable regions in two uninfarcted hearts was 0.057 ± 0.019. Panel 7K compares the infarct areas for all saline- and hpECM treated hearts using optical mapping. Consistent with histological analyses, the average infarct size is almost four times larger in saline- than in hpECM-treated hearts (8.5 vs. 2.3 mm^2), yet may under-represent the true infarct size for animals without a full thickness infarct, as only scars on the surface are captured with this imaging method.

4. Discussion

Heart disease remains the leading cause of mortality in the western world, with few therapeutic options available for treating the heart following an ischemic event [28]. Recently, hydrogels derived from decellularized non-human animal tissues, such as small intestinal submucosa (SIS), EHS tumor matrix, porcine myocardium, and pericardium have been investigated to repair the heart in animal models [9,14,29]. Surprisingly, successful therapeutic outcomes have been reported from the administration of the ECM alone (without cells); however, the risks associated with the use of xenograft hydrogel in the human heart, with possible alpha-gal contamination and subsequent immune system reactivity, may complicate the translation of these approaches to the clinic [14]. Furthermore, previous attempts to generate hydrogels from human tissues have shown significant variability in the final product characteristics and performance [14], likely due to donor variability in age and states of health and disease. This variability likely limits the clinical potential of these materials.

In this work, we assessed the potential of a solubilized human placental plate tissue-derived ECM preparation for cardiac cell culture applications *in vitro*, as well as therapeutic application in cell-free applications post myocardial infarction *in vivo*. hpECM preparations showed a high degree of consistency between the different lots tested (Fig. S3), with this material tested to be collagen-rich and laden with a large range of pro-regenerative, anti-scarring, and cell recruiting factors (e.g. VEGF [30], placental lactogen [31] and HGF [32]) (Supplementary Table 1). Additional growth factors unique to the placenta, such as IGF-II, which supports pancreatic islet cell differentiation in the fetus, and pro-angiogenic growth factor placental lactogen, were identified in hpECM (Table 1). hpECM preparations showed superior handling characteristics compared to other complex ECM preparations, as they did not require the use of chilled tools and equipment, forming a hydrogel at physiologic conditions yet remaining a liquid at room tempera-

Please cite this article in press as: M.P. Francis et al., Human placenta hydrogel reduces scarring in a rat model of cardiac ischemia and enhances cardiomyocyte and stem cell cultures, Acta Biomater. (2016), http://dx.doi.org/10.1016/j.actbio.2016.12.027

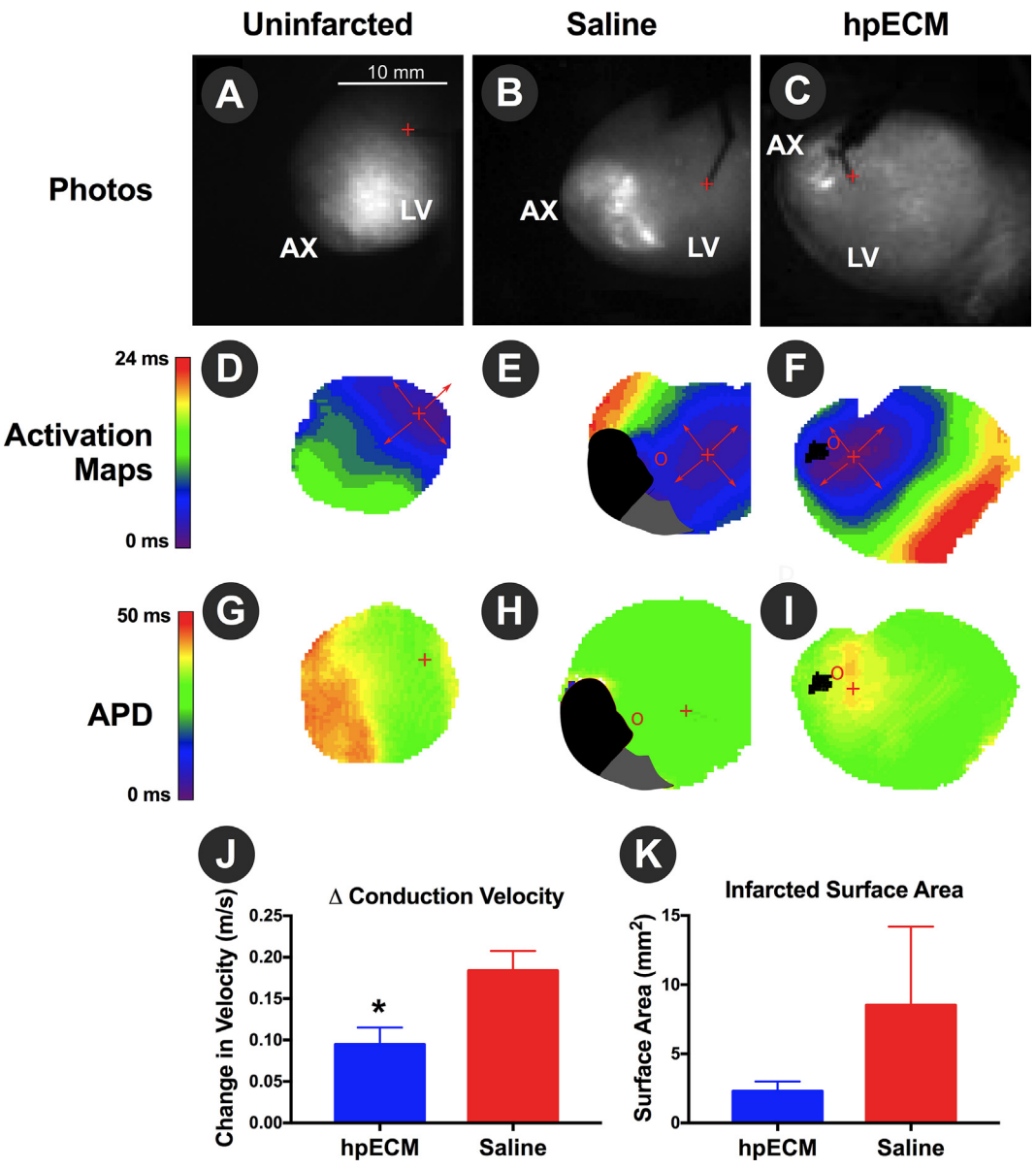

Fig. 7. Electrical Activity of Representative Infarct-free, Saline-treated, and hpECM-treated Rat Hearts. (A–C) Photographs of no-infarct (A), infarct-saline (B), and infarct-hpECM (C) hearts, with the apex (AX) and left ventricle (LV) noted for orientation. Besides the heart, the stimulation electrodes are visible, the location of stimulation is marked with a red "+". (D–F) Activation maps of no-infarct (D), infarct-saline (E), and infarct-hpECM (F) hearts. Every element of the cardiac surface is colored according to the time at which it was activated following stimulation at t = 0 ms (see the scale bar on the left). The stimulation site is marked with a red "+", the propagation of excitation away from the stimulation site is indicated by arrows. The ligation site for infarct creation are marked with a red circle in Panels (E) and (F). Black areas in (E) and (F) mark the infarcts in these hearts. Grey area in (E) could not be evaluated because of tissue adhesion following infarct surgery. (G–I) Action potential duration maps of no-infarct (G), infarct-saline (H), and infarct-hpECM (I) hearts. Every element of the cardiac surface is colored according to the local action potential duration (see the scale bar on the left), see Panels (D–F) for the meaning of other symbols. Variability of conduction velocity (J) was calculated to be significantly lower in hpECM-treated hearts than in saline-treated hearts ($p = 0.036$), while the average infarct size calculated by optical mapping is almost four times larger in saline- versus in hpECM-treated hearts (K). (For interpretation of the references to colour in this figure legend, the reader is referred to the web version of this article.)

ture, greatly facilitating its use. This hydrogel formed as a highly porous matrix with large, interconnected pores, as visualized by SEM (Fig. 1). Together, the ECM composition and growth factor complement along with favorable gelling characteristics make hpECM ideally suitable for a large number of cell culture, tissue engineering, and biomedical applications. Furthermore, the intact, decellularized placental plate, prior to solubilization as a hydrogel, and rather as a solid, may provide additional therapeutic utility, such as by providing a therapeutic void filler (e.g. a bridge material for repairing resected lymph nodes or other soft tissues).hpECM provided a suitable culture substrate for the of iPSC-derived cardiomyocytes, which allowed cells to attach, synchronize, and contract faster (around 1 Hz) on hpECM than on standard substrates (Figs. 2 and 3, and Videos 1, 2). This phenomenon has not been reported with other ECM hydrogel substrates and may have substantial impact *in vivo* and for diagnostic purposes. Improved cardiomyocyte culture system using hpECM may allow for more advanced cardiovascular cell culture studies for studying cardiac-related mechanisms (e.g. arrhythmia in 3D culture [33], or cardiac stem cell developmental pathways), and also for screening of pharmacologic agents and potential cardiotoxins [34]. hpECM further supported the culture of human somatic cardiomyocytes, showing no loss in metabolic activity over time in culture as compared to conventional used xenogenic ECMs (Fig. 2). As cellular therapies have matured, a move towards serum-free and xeno-free cultures has emerged as an ideal system as ensure safety and reproducibil-

Please cite this article in press as: M.P. Francis et al., Human placenta hydrogel reduces scarring in a rat model of cardiac ischemia and enhances cardiomyocyte and stem cell cultures, Acta Biomater. (2016), http://dx.doi.org/10.1016/j.actbio.2016.12.027

ity, with hpECM matrix thus presenting a compelling alternative to typical xenogenic matrices for translation cell therapies to the clinic. hpECM also supported the delivery of adipose stem cells (ASC) via a cardiac catheter without loss of viability (Fig. 2), providing further opportunities for the use of hpECM as a carrier for the site-directed application of cells in future, possible minimally invasive cellular therapies to the heart and also to other organs, using hpECM as the delivery vehicle. Furthermore, the rich specific ECM and growth factor composition of hpECM may provide promise for culture of additional cells or *in vivo* regenerative potential. For example, IGF-II in hpECM may promote pancreatic regeneration *in vivo* and support beta-islet cell culture, where FGF20 may promote survival of midbrain dopaminergic neurons.

In vivo, hpECM was found to be localized to the injection region as indicated by biotinlabeled hpECM (Fig. 5), and to persist after 2 weeks of subcutaneous injection (Fig. S1B). hpECM was localized in the interstitial space of the injected left ventricle at 1hr after delivery in live rats, as shown co-localized collagen staining via Sirius Red and biotin labeled-hpECM analyzed in serial heart sections (Fig. S1). Animal models and clinical studies have reported that therapeutic cells injected into the ischemic region rapidly migrate from the infarct and leave the heart in cases where the cells delivered without a scaffold carrier [2,3,35]. Thus, future use of hpECM may provide added therapeutic advantages by anchoring the cells at the injury site and act together to replace damaged cardiovascular tissue and inhibit scar formation.

Kaplan Meier mortality evaluation revealed no significant difference between hpECM treated and control animals, suggesting safety of the hpECM biomaterial. Only one animal was lost in hpECM injected group compared to 3 lost for saline injected controls. No adverse effects were observed via echocardiography in hpECM treated rats compared to controls. Ejection fraction, fractional shortening, end-systolic volume and end-diastolic volume measures were not significantly different between treatment groups. The occlusion in the distal region of the LAD resulted in a relatively small infarct size, which may account for minimal differences noticeable macroscopically via echocardiography. Histological evaluation of the injected region by H&E showing the absence of an inflammatory response in the hpECM injected rat at 8 weeks post-injection, as assessed by a pathologist, further suggest hpECM safety. hpECM significantly ($p = 0.0312$) reduced the average myocardial infarct size in treated vs saline injected rats, as quantitated in 8 week post-surgical rats (Fig. 5). Infarct size reduction was consistently shown with both Mason's Trichrome and TTC. Average infarct size in hpECM treated animals was 16 ± 5 mm^3 as compared to 45 ± 14 mm^3 in saline injected animals. H&E additionally revealed presence of cardiomyocytes in ischemic region distal to the LAD occlusion in hpECM treated animals, with no evidence of necrosis, inflammation, or increased myofibroblast cell density, thusly suggesting more viable cardiomyocytes present in hpECM treated animals, and indicating protection, repair or regeneration of the structural integrity of the myocardium.

Optical mapping experiments showed that hpECM not only increased the amount of surviving cardiac muscle tissue, but that this tissue was also fully functional from an electrophysiological point of view (Fig. 7). This finding is important, because insufficiently repaired tissue could lead to slow conduction, changes in action potential duration, and unidirectional block, which together could provide a substrate for arrhythmias that could be even worse than a larger infarct [36]. Induction of arrhythmia is a notable concern, as other approaches to restore ischemic myocardial tissue have reported aberrant electrical activity in the heart, including recent use of embryonic stem cell (ESC)-derived cardiomyocytes in primates [37]. No electrophysiological abnormalities were seen in any of the hpECM injected hearts, and the variability in conduction velocity was lower than for saline-treated hearts; both these findings suggest that the reduction of infarct size that hpECM does not come at the cost of arrhythmia risks. More importantly, these results further indicate that hpECM may support tissue repair and regeneration while reducing the default scar formation response, resulting in the functional recovery post-infarction.

5. Conclusions and significance

This is the first report describing the evaluation of an original, complex, human, xeno-free, tumor-material-free extracellular matrix hydrogel preparation isolated from human placentas, applied to myocardial applications, *in vitro* and *in vivo*. While placental plate has been decellularized previously, placenta has not been previously formed as a hydrogel as described here. We found that hpECM is rich in collagens, laminin, fibronectin, glycoproteins, and numerous growth factors, including known pro-regenerative, pro-angiogenic, anti-scarring, anti-inflammatory, and stem cell-recruiting factors. hpECM effectively supported the culture of cardiomyocytes, stem cells and HUVECs when compared to standard xenogeneic ECM materials. Assessed in a rat model of myocardial infarction, hpECM injections were safely deliverable to the ischemic myocardium, without deleterious effects in terms of mortality or cardiac function. hpECM injections in ischemic myocardium resulted in significant reduction in infarct size, more viable myocardium, and a normal electrophysiological contraction profile. Human placenta-derived ECM hydrogels have potential in therapeutic cardiovascular regenerative medicine applications, and is a promising substratum for basic cell-based research in this biomimetic 3D human tissue-derived extracellular matrix environment.

Disclosures

Funding: This work was supported by the non-profit, LifeNet Health. Authors: MF, EB, RR, RO, SC and AH are or were previously employed by LifeNet Health. All studies were designed by MF, except for optical mapping studies (by CZ, FV and MF), and mass spectrometry studies (by SD and MF), with data collected, analyzed, and interpreted by all authors, and the manuscript composed by MF. The authors have no direct financial interest in the publication of this work.

Appendix A. Supplementary data

Supplementary data associated with this article can be found, in the online version, at http://dx.doi.org/10.1016/j.actbio.2016.12.027.

References

[1] I Perea-Gil, C Prat-Vidal, A. Bayes-Genis, In vivo experience with natural scaffolds for myocardial infarction: the times they are a-changin, Stem Cell Res. Ther. 6 (1) (2015), http://dx.doi.org/10.1186/s13287-015-0237-4. 248-015-0237-4.

[2] R. Vogel, E.A. Hussein, S.A. Mousa, Stem cells in the management of heart failure: what have we learned from clinical trials?, Expert Rev Cardiovasc. Ther. 13 (1) (2015) 75–83, http://dx.doi.org/10.1586/14779072.2015.988142.

[3] A.R. Chugh, G.M. Beache, J.H. Loughran, N. Mewton, J.B. Elmore, J. Kajstura, P. Pappas, A. Tatooles, M.F. Stoddard, J.A. Lima, M.S. Slaughter, P. Anversa, R. Bolli, Administration of cardiac stem cells in patients with ischemic cardiomyopathy: the SCIPIO trial: surgical aspects and interim analysis of myocardial function and viability by magnetic resonance, Circulation 126 (11 Suppl 1) (2012) S54–S64. 126/11_suppl_1/S54 [pii].

[4] R. Bolli, A.R. Chugh, D. D'Amario, J.H. Loughran, M.F. Stoddard, S. Ikram, G.M. Beache, S.G. Wagner, A. Leri, T. Hosoda, F. Sanada, J.B. Elmore, P. Goicherg, D. Cappeta, N.K. Solankhi, I. Fahsah, D.G. Rokosh, M.S. Slaughter, J. Kajstura, P. Anversa, Cardiac stem cells in patients with ischaemic cardiomyopathy (SCIPIO): initial results of a randomised phase 1 trial, Lancet 378 (9806) (2011) 1847–1857, http://dx.doi.org/10.1016/S0140-6736(11)61590-0.

[5] V. Bellamy, V. Vanneaux, A. Bel, H. Nemetalla, S. Emmanuelle-Boitard, Y. Farouz, P. Joanne, M.C. Perier, E. Robidel, C. Mandet, A. Hagège, P. Bruneval, J. Larghero, O. Agbulut, P. Menasché, Long-term functional benefits of human embryonic stem cell-derived cardiac progenitors embedded into a fibrin scaffold, J. Heart Lung Transplant. 34 (9) (2015) 1198–1207, http://dx.doi.org/10.1016/j.healun.2014.10.008.

[6] T. Narita, Y. Shintani, C. Ikebe, M. Kaneko, N.G. Campbell, S.R. Coppen, R. Uppal, Y. Sawa, K. Yashiro, K. Suzuki, The use of scaffold-free cell sheet technique to refine mesenchymal stromal cell-based therapy for heart failure, Mol. Ther. 21 (4) (2013) 860–867, http://dx.doi.org/10.1038/mt.2013.9.

[7] C. Gallina, V. Turinetto, C. Giachino, A new paradigm in cardiac regeneration: The mesenchymal stem cell secretome, Stem Cells Int. 2015 (2015) 765846, http://dx.doi.org/10.1155/2015/765846.

[8] M.L. Liu, T. Nagai, M. Tokunaga, K. Iwanaga, K. Matsuura, T. Takahashi, M. Kanda, N. Kondo, A.T. Naito, I. Komuro, Y. Kobayashi, Anti-inflammatory peptides from cardiac progenitors ameliorate dysfunction after myocardial infarction, J. Am. Heart Assoc. 3 (6) (2014) e001101, http://dx.doi.org/10.1161/JAHA.114.001101.

[9] J.M. Singelyn, J.A. DeQuach, S.B. Seif-Naraghi, R.B. Littlefield, P.J. Schup-Magoffin, K.L. Christman, Naturally derived myocardial matrix as an injectable scaffold for cardiac tissue engineering, Biomaterials 30 (29) (2009) 5409–5416, http://dx.doi.org/10.1016/j.biomaterials.2009.06.045.

[10] Seif-Naraghi SB, Singelyn JM, Salvatore MA, Osborn KG, Wang JJ, Sampat U, Kwan OL, Strachan GM, Wong J, Schup-Magoffin PJ, Braden RL, Bartels K, DeQuach JA, Preul M, Kinsey AM, DeMaria AN, Dib N, and Christman KL. Safety and efficacy of an injectable extracellular matrix hydrogel for treating myocardial infarction. Sci Transl Med. 2013;5(173):173ra25. doi: http://dx.doi.org/10.1126/scitranslmed.3005503 [doi].

[11] L. Ou, W. Li, Y. Zhang, J. Liu, H. Sorg, D. Furlani, R. Gäbel, P. Mark, C. Klopsch, L. Wang, K. Lützow, A. Lendlein, K. Wagner, D. Klee, A. Liebold, R.K. Li, D. Kong, G. Steinhoff, N. Ma, Intracardiac injection of matrigel induces stem cell recruitment and improves cardiac functions in a rat myocardial infarction model, J. Cell Mol. Med. 15 (6) (2011) 1310–1318, http://dx.doi.org/10.1111/j.1582-4934.2010.01086.x.

[12] C.G. McGregor, H. Kogelberg, M. Vlasin, G.W. Byrne, Gal-knockout bioprostheses exhibit less immune stimulation compared to standard biological heart valves, J. Heart Valve Dis. 22 (3) (2013) 383–390.

[13] T. Wilhite, C. Ezzelarab, H. Hara, C. Long, D. Ayares, D.K. Cooper, M. Ezzelarab, The effect of gal expression on pig cells on the human T-cell xenoresponse, Xenotransplantation 19 (1) (2012) 56–63, http://dx.doi.org/10.1111/j.1399-3089.2011.00691.x.

[14] T.D. Johnson, J.A. Dequach, R. Gaetani, J. Ungerleider, D. Elhag, V. Nigam, A. Behfar, K.L. Christman, Human versus porcine tissue sourcing for an injectable myocardial matrix hydrogel, Biomater. Sci. 2014 (2014) 60283D, http://dx.doi.org/10.1039/C3BM60283D.

[15] O'Connor DM, Naresh NK, Piras BA, Xu Y, Smith RS, Epstein FH, Hossack JA, Ogle RC, French BA. A novel cardiac muscle-derived biomaterial reduces dyskinesia and postinfarct left ventricular remodeling in a mouse model of myocardial infarction. Physiol Rep. 2015;3(3):10.14814/phy2.12351. doi: http://dx.doi.org/10.14814/phy2.12351 [doi].

[16] K.G. Cornwell, A. Landsman, K.S. James, Extracellular matrix biomaterials for soft tissue repair, Clin. Podiatr. Med. Surg. 26 (4) (2009) 507–523, http://dx.doi.org/10.1016/j.cpm.2009.08.001.

[17] J.S. Kim, J.C. Kim, B.K. Na, J.M. Jeong, C.Y. Song, Amniotic membrane patching promotes healing and inhibits proteinase activity on wound healing following acute corneal alkali burn, Exp. Eye Res. 70 (3) (2000) 329–337, http://dx.doi.org/10.1006/exer.1999.0794.

[18] Y. Hao, D.H. Ma, D.G. Hwang, W.S. Kim, F. Zhang, Identification of antiangiogenic and antiinflammatory proteins in human amniotic membrane, Cornea 19 (3) (2000) 348–352.

[19] S.C. Tseng, D.Q. Li, X. Ma, Suppression of transforming growth factor-beta isoforms, TGF-beta receptor type II, and myofibroblast differentiation in cultured human corneal and limbal fibroblasts by amniotic membrane matrix, J. Cell. Physiol. 179 (3) (1999) 325–335, http://dx.doi.org/10.1002/(SICI)1097-4652(199906)179:3<325::AID-JCP10>3.0.CO;2-X.

[20] M. Litwiniuk, T. Grzela, Amniotic membrane: new concepts for an old dressing, Wound Repair Regen. 22 (4) (2014) 451–456, http://dx.doi.org/10.1111/wrr.12188.

[21] A.C. Mamede, M.J. Carvalho, A.M. Abrantes, M. Laranjo, C.J. Maia, M.F. Botelho, Amniotic membrane: from structure and functions to clinical applications, Cell Tissue Res. 349 (2) (2012) 447–458, http://dx.doi.org/10.1007/s00441-012-1424-6.

[22] Y.P. Talmi, L. Sigler, E. Inge, Y. Finkelstein, Y. Zohar, Antibacterial properties of human amniotic membranes, Placenta 12 (3) (1991) 285–288. 0143-4004(91)90010-D [pii].

[23] A. Silini, O. Parolini, B. Huppertz, I. Lang, Soluble factors of amnion-derived cells in treatment of inflammatory and fibrotic pathologies, Curr. Stem Cell Res. Ther. 8 (1) (2013) 6–14. CSCRT-EPUB-20121224-5 [pii].

[24] L. Yang, S.M. Dutta, D.A. Troyer, J.B. Lin, R.A. Lance, J.O. Nyalwidhe, R.R. Drake, O.J. Semmes, Dysregulated expression of cell surface glycoprotein CDCP1 in prostate cancer, Oncotarget 6 (41) (2015) 43743–43758, http://dx.doi.org/10.18632/oncotarget.6193.

[25] I. Semenov, S. Xiao, A.G. Pakhomov, Primary pathways of intracellular ca(2+) mobilization by nanosecond pulsed electric field, Biochim. Biophys. Acta 1828 (3) (2013) 981–989, http://dx.doi.org/10.1016/j.bbamem.2012.11.032.

[26] W.R. Mills, N. Mal, F. Forudi, Z.B. Popovic, M.S. Penn, K.R. Laurita, Optical mapping of late myocardial infarction in rats, Am. J. Physiol. Heart Circ. Physiol. 290 (3) (2006) H1298–H1306. 00437.2005 [pii].

[27] I.R. Efimov, V.P. Nikolski, G. Salama, Optical imaging of the heart, Circ. Res. 95 (1) (2004) 21–33, http://dx.doi.org/10.1161/01.RES.0000130529.18016.35.

[28] Mozaffarian D, Benjamin EJ, Go AS, Arnett DK, Blaha MJ, Cushman M, de Ferranti S, Després JP, Fullerton HJ, Howard VJ, Huffman MD, Judd SE, Kissela BM, Lackland DT, Lichtman JH, Lisabeth LD, Liu S, Mackey RH, Matchar DB, McGuire DK, Mohler ER 3rd, Moy CS, Muntner P, Mussolino ME, Nasir K, Neumar RW, Nichol G, Palaniappan L, Pandey DK, Reeves MJ, Rodriguez CJ, Sorlie PD, Stein J, Towfighi A, Turan TN, Virani SS, Willey JZ, Woo D, Yeh RW, Turner MB; American Heart Association Statistics Committee and Stroke Statistics Subcommittee. Heart disease and stroke statistics–2015 update: A report from the american heart association. Circulation. 2015;131(4):e29-322. doi: http://dx.doi.org/10.1161/CIR.0000000000000152 [doi].

[29] A.J. Rufaihah, D. Seliktar, Hydrogels for therapeutic cardiovascular angiogenesis, Adv. Drug Deliv. Rev. (2015). S0169-409X(15)00156-8 [pii].

[30] J.E. Lahteenvuo, M.T. Lahteenvuo, A. Kivela, C. Rosenlew, A. Falkevall, J. Klar, T. Heikura, T.T. Rissanen, E. Vähäkangas, P. Korpisalo, B. Enholm, P. Carmeliet, K. Alitalo, U. Eriksson, S. Ylä-Herttuala, Vascular endothelial growth factor-B induces myocardium-specific angiogenesis and arteriogenesis via vascular endothelial growth factor receptor-1- and neuropilin receptor-1-dependent mechanisms, Circulation 119 (6) (2009) 845–856, http://dx.doi.org/10.1161/CIRCULATIONAHA.108.816454.

[31] A.M. Corbacho, G. Martinez De La Escalera, C. Clapp, Roles of prolactin and related members of the prolactin/growth hormone/placental lactogen family in angiogenesis, J. Endocrinol. 173 (2) (2002) 219–238. JOE04352 [pii].

[32] S.B. Sonnenberg, A.A. Rane, C.J. Liu, N. Rao, G. Agmon, S. Suarez, R. Wang, A. Munoz, V. Bajaj, S. Zhang, R. Braden, P.J. Schup-Magoffin, O.L. Kwan, A.N. DeMaria, J.R. Cochran, K.L. Christman, Delivery of an engineered HGF fragment in an extracellular matrix-derived hydrogel prevents negative LV remodeling post-myocardial infarction, Biomaterials 45 (2015) 56–63, http://dx.doi.org/10.1016/j.biomaterials.2014.12.021.

[33] Y.W. Chiu, W.P. Chen, C.C. Su, Y.C. Lee, P.H. Hsieh, Y.L. Ho, The arrhythmogenic effect of self-assembling nanopeptide hydrogel scaffolds on neonatal mouse cardiomyocytes, Nanomedicine 10 (5) (2014) 1065–1073, http://dx.doi.org/10.1016/j.nano.2014.01.005.

[34] F. Pampaloni, E.H. Stelzer, A. Masotti, Three-dimensional tissue models for drug discovery and toxicology, Recent Pat. Biotechnol. 3 (2) (2009) 103–117.

[35] E.T. Roche, C.L. Hastings, S.A. Lewin, D.E. Shvartsman, Y. Brudno, N.V. Vasilyev, F.J. O'Brien, C.J. Walsh, G.P. Duffy, D.J. Mooney, Comparison of biomaterial delivery vehicles for improving acute retention of stem cells in the infarcted heart, Biomaterials 35 (25) (2014) 6850–6858, http://dx.doi.org/10.1016/j.biomaterials.2014.04.114.

[36] A.L. Wit, M.R. Rosen, Pathophysiologic mechanisms of cardiac arrhythmias, Am. Heart J. 106 (4 Pt 2) (1983) 798–811.

[37] J.J. Chong, X. Yang, C.W. Don, E. Minami, Y.W. Liu, J.J. Weyers, W.M. Mahoney, B. Van Biber, S.M. Cook, N.J. Palpant, J.A. Gantz, J.A. Fugate, V. Muskheli, G.M. Gough, K.W. Vogel, C.A. Astley, C.E. Hotchkiss, A. Baldessari, L. Pabon, H. Reinecke, E.A. Gill, V. Nelson, H.P. Kiem, M.A. Laflamme, C.E. Murry, Human embryonic-stem-cell-derived cardiomyocytes regenerate non-human primate hearts, Nature 510 (7504) (2014) 273–277, http://dx.doi.org/10.1038/nature13233.

Please cite this article in press as: M.P. Francis et al., Human placenta hydrogel reduces scarring in a rat model of cardiac ischemia and enhances cardiomyocyte and stem cell cultures, Acta Biomater. (2016), http://dx.doi.org/10.1016/j.actbio.2016.12.027